Intermediate Phase in Molecular Networks and Solid Electrolytes

M. Micoulaut[1]

There is growing evidence that electronic and molecular networks present some common universal properties, among which is the existence of a self-organized intermediate phase. In glasses, the latter is revealed by the reversibility window obtained from complex calorimetric measurements at the glass transition. Here we focus on amorphous networks and we show how this intermediate phase can be understood from a rigidity percolation analysis on size increasing clusters. This provides benchmarks and guidance for an electromechanical analogy with high temperature superconductors.

KEY WORDS: self-organization; molecular networks; conductivity.

1. INTRODUCTION

In the recent years, more and more studies devoted to the understanding of the metal–insulator transition (MIT) have stressed the possible existence of a self-organized electronic phase [1,2] that may explain the superconducting state. In these studies, in addition to the prediction or the measurement of a critical dopant concentration n_{c1}, it is noteworthy to stress that although the mobile charge carrier concentration should tend to zero at the MIT and therefore also the interaction between the carriers, the temperature T_c ... should tend to zero, in contrast with current observation. Moreover, a second anomalous behavior is observed at a concentration n_{c2} from the superconductive phase to the nonsuperconductive Fermi liquid. This second transition is much more abrupt and seems first order in character [3]. Illustrative examples of these behaviors can be found in LSCO ($La_{2-x}Sr_xCuO_4$) from measurements of the filling factors by Meissner volume (i.e. measuring the fraction of the material that is superconductive) and the transition temperature $T_c(x)$ with respect to Sr concentration [4]. The nature of this intermediate phase in the

dopant region $n_{c1} < n < n_{c2}$ therefore still needs to be understood. However, beyond the details of modelling [6], a general consensus emerge, which puts forward the idea of the formation of modulated spatial patterns of mesoscopic length scale as being responsible for HTSC [2,5].

Much more simpler examples of self-organization and the existence of an intermediate phase can be provided by network glasses [6]. Here, instead of following the concentration of mobile carriers, focus is made on elastic deformations of an amorphous network. Thus, instead of MIT, percolative stiffness transitions [7] are obtained upon changing the number of possible deformations, which, in turn, can be related to the connectivity of the molecular network. In order to describe these deformations, one simple and elegant idea is to translate the covalent interatomic valence forces of the atoms in bond-stretching and bond-bending mechanical constraints (n_c^α and n_c^β), using (mean-field) Maxwell constraint counting [8]. A very particular point is reached when the number of mechanical constraints $n_c = n_c^\alpha + n_c^\beta$ per atom equals the degrees of freedom per atom in 3D, i.e. $n_c = 3$ (corresponding to optimal glass formation) [9]. This result has been obtained independently from rigidity percolation by Thorpe [10] on disordered networks, showing that the number of zero frequency solutions (floppy modes)

[1]Laboratoire de Physique Théorique des Liquides, Universite Pierre et Marie Curie, Boite 121, 4, place Jussieu 75252 Paris Cedex 05, France.

f of the dynamical matrix of the network equals $f = 3 - n_c$. The enumeration of constraints has been performed on a network of N atoms composed of n_r atoms that are r-fold coordinated, yielding $n_c^\alpha = r/2$ bond-stretching constraints and $n_c^\beta = 2r - 3$ bond-bending constraints for a r-fold coordinated atom. The vanishing of the number of floppy modes is obtained when the mean coordination number of the network reaches the critical value of 2.4, identified with an elastic stiffness transition [11]. This point defines the transition between a floppy network that can be deformed without any cost in energy and a stressed rigid network that has more constraints than degrees of freedom. At the mean coordination number of 2.4, the network is isostatic. This new phase transition has been studied with considerable success in chalcogenides both in experiments and numerical simulations [12]. Applications of rigidity theory have also been reported in various fields such as granular matter, biology, and computational science [13]. However, in the more recent years it has been shown that there should be two transitions [14] instead of the previously reported single transition, suggesting that the mean-field constraint counting alone may be insufficient to describe completely the network change. Results on Raman scattering and measurements of the kinetics of the glass transition using modulated differential scanning calorimetry (MDSC) have indeed provided evidence [14,15] for two vibrational thresholds, thus defining a stress-free intermediate phase (isostatically rigid) in between the floppy and the stressed rigid phases, for which independent evidence is obtained from numerical simulations [16].
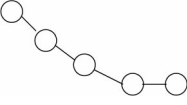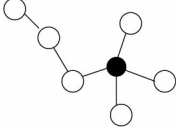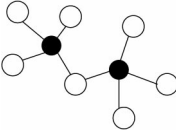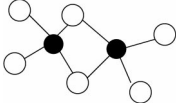
In this paper, we will construct a systematic approach that enables us to perform constraint counting on size increasing structures, thus permitting to take into account medium range order effects such as small rings. In doing this, we show that these small rings mostly control the values of the critical coordination numbers and the width of the intermediate phase. The construction will also show how isostatic regions and self-organization influence the absolute magnitude of the width. The simplest case that can be build up corresponds to Group IV chalcogenide glasses of the form $B_x A_{1-x}$ with coordination numbers $r_A = 2$ and $r_B = 4$ defining the mean coordination number $\bar{r} = 2 + 2x$. Size-increasing cluster approximations (SICA) have been used in order to generate medium range order (MRO) from sets of clusters on which we have realized constraint counting. The results show two transitions. A first one at which

the number of floppy modes vanishes and a second one (a "stress transition") beyond which stress in the structure cannot be avoided anymore out of ring structures. In between, this defines an almost stress-free network structure for which the rate of isostatic regions can be computed. We will extend these results on solid electrolytes for which percolative conductivity should be detected.

2. SIZE INCREASING CLUSTER APPROXIMATIONS AND CONSTRAINT COUNTING

Size increasing cluster approximations (SICA) has been first introduced to describe the medium and intermediate range order in amorphous semiconductors [17] but their usefulness has also been stressed for the description of the formation of quasi-crystals [18] and fullerenes [19]. This approach emphasizes the rapid convergence of significant MRO structures to a limit value when the size of the considered clusters is increasing. Ideally, the infinite size cluster distribution would yield the exact statistics of MRO in the structure. The construction of these clusters is realized in Canonical Ensemble, with particular energy levels corresponding to bond creation between short range order molecules (basic units) that are used as building blocks from step $l = 1$ (corresponding here to the reported mean-field approach [8]) to arbitrary. This construction should be realized at the formation of the network, when T equals the fictive temperature T_f [20]. Since we expect to relate the width of the intermediate phase with the ring fraction, we will restrict our present study to Group IV chalcogenides of the form $Si_x Se_{1-x}$. For the latter, there is strong evidence that at the stoichiometric concentration $x = 0.33$ a substantial amount of edge-sharing $SiSe_{4/2}$ tetrahedra [21] can be found. Therefore, we select basic units such as the A_2 (i.e. Se_2) chain fragment and the stoichiometric $BA_{4/2}$ molecule (i.e. $SiSe_{4/2}$). These basic units have respective probabilities $1 - p$ and $p = 2x/(1 - x)$, x being the concentration of the Group IV atoms. We associate the creation of a chain-like $A_2 - A_2$ structure (see Table I) with an energy state of E_1, isostatic $A_2 - BA_2$ bondings with an energy gain of E_2, and corner-sharing (CS) and edge-sharing (ES) $BA_{4/2}$ tetrahedra or any ring structure respectively with E_3 and E_4. The probabilities of the different clusters have statistical weights $g(E_i)$ that can be regarded as the degeneracy of the corresponding energy level and correspond to the number of equivalent ways a cluster can be constructed.

Table I. The Four Clusters Generated at Step $l = 2$ With Their Unrenormalized Probabilities and Their Number of Mechanical Constraints[a]

Symbol	Mechanical nature		Probabilty	n_c
A_4	Flopy		$4(1-p)e_1^2$	2.0
BA_4	Isostatic		$16p(1-p)e_2$	3.0
B_2A_4	Stressed		$16p^2e_3$	3.67
B_2A_2	Stressed		$72p^2e_4$	3.33

[a]The factors e_i are Boltzmann factors involving bond energies and the fictive temperature, $e_i = \exp[-E_i/T_f]$.

Examples of statistical weights for the step $l = 2$ are shown in Table I and in Refs. [17,18].

Because of the initial choice of the basic units, the energy E_2 will mostly determine the probability of isostatic clusters since this quantity is involved in the probability of creating the isostatic BA_4 cluster (a $A_2 - BA_{4/2}$ bonding). As a consequence, if we have $E_2 \ll E_1, E_3, E_4$, the network will be mainly isostatic in the range of interest.

The calculation of the number of bond-bending and bond-stretching mechanical constraints (n_c^β and n_c^β) per atom is performed on each cluster by Maxwell counting, and redundant constraints in ring structures are removed following the procedure described by Thorpe [10]. It is obvious from the construction that all the cluster probabilities will depend only on two parameters (i.e. the factors e_1/e_2 and e_3/e_2) and eventually e_4/e_2 if one considers the possibility of ES tetrahedra or rings. One of the two factors has to be composition dependent since a conservation law for the concentration of B atoms $x^{(l)}$ has to be fulfilled at any step l of the construction [22]:

$$x^{(l)} = x \quad (1)$$

This means that either the fictive temperature T_f or the energies E_i depend on x [20] but here only the $e_i(x)$ dependence is relevant for our purpose. Of course, when the step l will increase, the number of isomers will also increase, and among those, also the number of different types of rings. The construction has been realized up to the step $l = 4$, which already creates clusters of MRO size. For each step l, we have determined either e_1/e_2 or e_3/e_2 solving Eq. (1) and computed the total number of constraints n_c^l:

$$n_c^l = \frac{\sum_{i=1}^{N_l} n_{c(i)} p_i}{\sum_{i=1}^{N_l} N_i p_i} \quad (2)$$

where $n_c(i)$ and N_i respectively are the number of constraints and the number of atoms of the cluster of size l with probability p_i. Once the factors become composition dependent, it is possible to find for which concentration x (or which mean coordination number $\bar{r}$) the system reaches an optimal glass formation where the number of floppy modes $f = 3 - n_c^l$ vanishes.

3. RESULTS

Various possibilities can be studied within this framework. The simplest case that can be investigated at the very beginning is the random bonding case, which is obtained when the cluster probabilities p_i
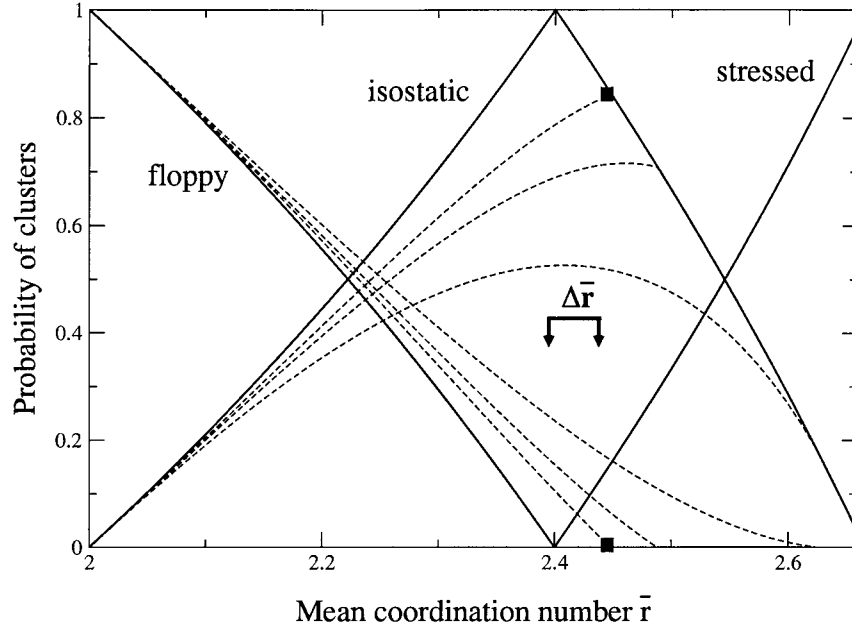
Fig. 1. Probability of finding floppy, isostatic rigid, and stressed rigid clusters as a function of mean coordination number $\bar{r}$ at SICA step $l = 2$ for different fractions of edge-sharing. The solid line corresponds to the dendritic case where no rings are allowed ($e_4 = 0$). The broken lines correspond to situations with a fraction of ES at the stress transition of $\eta = 0.156, 0.290$, and 0.818. The filled squares indicate the point $\bar{r}_{c2}$ at which the stress transition occurs in the case $\eta = 0.156$

are given only by their statistical weights (in other words, the factors e_i are set to 1). A single solution is obtained for the glass optimum point defined by $f = 0$ at all SICA steps, in the mean coordination number range [2.231, 2.275], slightly lower than the usual mean-field value of 2.4. Since there is only one solution, no intermediate phase in the case of random bonding is found.

Self-organization can be obtained by starting from a floppy cluster of size l (e.g. a chain-like structure made of a majority of A atoms), and allowing the agglomeration of a new basic unit onto this cluster to generate the cluster of size $l + 1$ only if the creation of a stressed rigid region can be avoided on this new cluster. The latter occurs when two $BA_{4/2}$ basic units are joined together. With this rather simple rule, upon increasing $\bar{r}$ one accumulates isostatic rigid regions on the size increasing clusters because $BA_{4/2}$ units are accepted only in $A_2 - BA_{4/2}$ isostatic bondings with energy E_2. Alternatively, we can start from a stressed rigid cluster, which exist at a higher mean coordination number ($\bar{r} \leq 2.67$), and follow the same procedure but in an opposite way, i.e. we allow only those bondings that lead to isostatic rigid regions, excluding systematically the possibility of floppy $A_2 - A_2$ bond-

ings. In the case of self-organized clusters, the simplest case to be studied is the case of dendritic clusters, when ring creation is avoided. For an infinite size l, this would permit to recover the results from Bethe lattice solutions or Random Bond Models [23] for which rings are also exluded in the thermodynamic limit [24]. A single transition for even l steps at exactly the mean-field value $\bar{r} = 2.4$ is obtained whereas for the step $l = 3$, there is a sharp intermediate phase defined by $f = 0$ (still at $\bar{r} = 2.4$) and the vanishing of floppy regions (i.e. e_1/e_2 is zero) at $\bar{r} = 2.382(6)$. The probability of floppy, isostatic rigid, and stressed rigid clusters as a function of the mean coordination number has been computed and shows that the network is entirely isostatic at the point where $f = 0$ (solid line, Fig. 1).

The intermediate phase shows up if a certain amount of MRO is allowed. This is realized in the SICA construction by setting the quantity e_4/e_2 nonzero, i.e. ES tetrahedra $BA_{4/2}$ leading to four-membered rings B_2A_4 can now be created at the growing cluster steps. Two transitions are now obtained for every SICA step. The first one is still located at $\bar{r}_{c1} = 2.4$ (see Fig. 1). There, the number of floppy modes f vanishes. The second one is located at $\bar{r}_{c2}$. When starting from a floppy network close to $\bar{r} = 2$
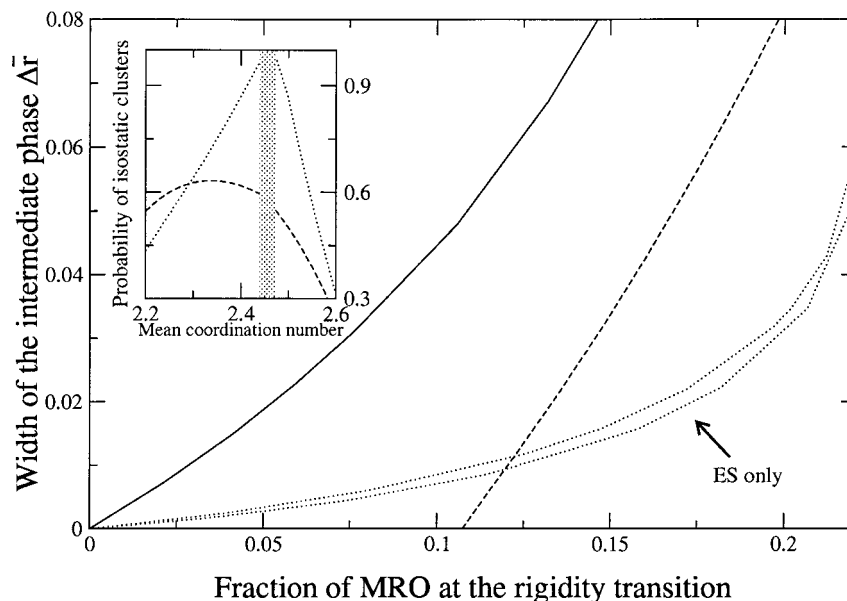
Fig. 2. Width of the intermediate phase $\Delta \bar{r}$ as a function of the fraction of ring clusters at the rigidity transition for $l = 2$ (solid line), $l = 3$ (dashed line) and $l = 4$ (dotted lines). At step $l = 2$, the nonzero width comes only from the edge-sharing $BA_{4/2}$ tetrahedra. For $l > 2$, different rings sizes $(4, 6, 8)$ have been taken into account. The lower dotted line corresponds to the intermediate phase at $l = 4$ if only ES are allowed as stressed rigid fragments. The upper dotted line is the same quantity but allowing any ring structure. The insert shows the probability of isostatic clusters with mean coordination number $\bar{r}$ for $l = 4$ (dotted line) and $l = 3$ (dashed line). The shaded region of $l = 4$ represents the intermediate phase.

and requiring self-organization (in this case, allowing only floppy or isostatic bondings), this point corresponds to the network composition beyond which stressed rigid regions outside of ring structures, which are created by the dendritic connection of at least two $BA_{4/2}$ units, cannot be avoided anymore. We call this point the "stress transition." We show in Fig. 1 the $l = 2$ result where $f = 0$ at $\bar{r}_{c1} = 2.4$ for different fractions of ES tetrahedra, defining an intermediate phase $\Delta \bar{r}$. It is noteworthy to stress that the first transition at $\bar{r}_{c1}$ corresponding to Phillips' glass optimum does not depend on the ES fraction, as well as on the fraction of stressed rigid clusters in the structure. To ensure continuous deformation of the network when B atoms are added and keeping the sum of the probability of floppy, isostatic rigid, and stressed rigid clusters equal to 1, the probability of isostatic rigid clusters connects the isostatic solid line at $\bar{r}_{c2}$. Stressed rigid rings first appear in the region $\bar{r}_{c1} < \bar{r} < \bar{r}_{c2}$ while chain-like stressed clusters (whose probability is proportional to e_3) occur only beyond the stress transition, when $e_3 \neq 0$. This means that within this approach, when $\bar{r}$ is increased, stressed rigidity nucleates through the network starting from rings, as ES tetrahedra. It appears

from Fig. 1 that the width $\Delta \bar{r} = \bar{r}_{c2} - \bar{r}_{c1}$ of the intermediate phase increases with the fraction of ES. We have represented the width as a function of the overall MRO fraction at the rigidity transition in Fig. 2, which shows that $\Delta \bar{r}$ is almost an increasing function of the ES fraction as seen from the result at SICA step $l = 4$. Here, there is only a small difference between allowing only four-membered rings (ES) (lower dotted line) or rings of all sizes (upper dotted line) in the clusters. Concerning the nature of the structure in the intermediate phase, one can see from Fig. 1 and the insert of Fig. 2 that the probability of isostatic clusters is maximum in the window $\Delta \bar{r}$, and almost equal to 1 for the even SICA steps, providing evidence that the molecular structure in the window is almost stress-free. Furthermore, the latter can be extremely broad if a high amount of ES is allowed. For a fraction of ES, η is close to 1, molecular stripes emerge in the structure that are isostatic, and every addition of new B atoms lowers the amount of remaining A-chains by converting them in ES $BA_{4/2}$ stripes. These molecular stripes are stress-free only if their size is infinite [10], which is the case for $\eta \simeq 1$ in the thermodynamic limit.

4. APPLICATION TO CHALCOGENIDES

As mentioned above, chalcogenide glasses are the first systems that have been carefully studied in the context of self-organization. SICA therefore provides a benchmark to check the results obtained. To be specific, Raman scattering has been used [25,26] as a probe to detect elastic thresholds in binary Si_xSe_{1-x} and Ge_xSe_{1-x} or ternary $Ge_xAs_xSe_{1-2x}$ glasses [27]. Changes in the germanium or silicon corner sharing mode chain frequencies have been studied with mean coordination number $\bar{r}$ of the glass network. These frequencies exhibit a change in slope at the mean coordination number $\bar{r}_{c1} = 2.4$ and a first-order jump at the second transition $\bar{r}_{c2}$. In germanium systems, the second transition is located around the mean coordination number of 2.52 whereas $\bar{r}_{c2} = 2.54$ in Si-based systems. For both systems, a power-law behavior in $\bar{r} - \bar{r}_{c2}$ is detected for $\bar{r} > \bar{r}_{c2}$ and the corresponding measured exponent is very close to the one obtained in numerical simulations of stressed rigid networks [28]. Moreover, a clear correlation between these results and the vanishing of the nonreversing heat flow ΔH_{nr} (the part of the heat flow that is thermal history sensitive) in MDSC measurements has been shown [25,26].

The SICA approach shows that the width $\Delta \bar{r}$ of the intermediate phase increases mostly with the fraction of ES tetrahedra. We stress that the width should converge to a lower limit value of $\Delta \bar{r}$ compared to the step $l = 2$, and therefore one can observe the shift downwards when increasing l from 2 to 4. This limit value is in principle attained for $l \to \infty$, or at least for much larger steps than $l = 4$ [29]. For Si–Se, $\Delta \bar{r} = 0.14$ is somewhat larger than for Ge–Se ($\Delta \bar{r} = 0.12$), consistent with the fact that the number of ES is higher in the former [26].

5. APPLICATION TO SOLID ELECTROLYTES

One interesting field of application of cluster construction and constraint counting algorithms is the area of fast ionic conductors (FIC) [30,31], which has recently gained attention because of potential applications of these solid electrolytes in all solid state electrochemical devices and/or miniaturized systems such as solid state batteries. This has been made possible by substitution of more polarizable sulfur atoms, replacing the oxygen in usual oxide glasses, and has led to a substantial increase of the conductivity [32], as high as $10^{-3} \, \Omega^{-1} \, cm^{-1}$, three orders of magnitude higher than
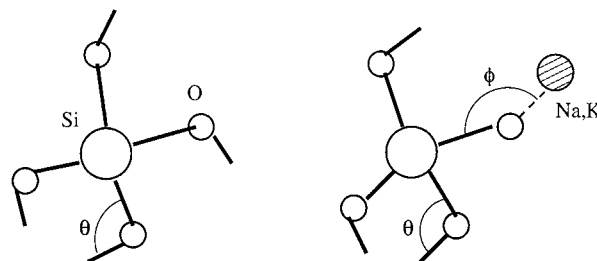

Fig. 3. The two local structures of the fast ionic conducting $(1 - x)SiX_2 - xM_2X$, ($X = O, S, Se$; $M = Li, Na, K$) glasses, denoted as Q_4 and Q_3 units, with respective probabilities $1 - p$ and $p = 2x/(1 - x)$.

the conductivity of analogous oxide glasses [33]. Surprisingly, the extension of constraint theory from network glasses (as Si_xSe_{1-x}) to FIC has been reported only for a few oxide glasses [34,35]. As a consequence, percolative effects have not been studied so far with the network change in FIC's, although it seems fundamental for the understanding of the mobile alkali cations' motion. Since the conductivity of the semiconductor is proportional to the mobility μ, which, in turn, is related to the deformation of the network [36], and the free carrier concentration n_L by $\sigma = \mu n_L e$, one may expect that the mobility in a floppy FIC should be substantially higher compared to the cation mobility in a stressed rigid network. This means that the conductivity σ should display some particular behavior in the stress-free intermediate phase and at the two transitions.

One can extend the SICA approach to the present case by considering the simplest binary conducting glass, which is of the form $(1 - x)SiX_2 - xM_2X$, with X an atom of Group VI ($X = O, S, Se$) and M an alkali cation (M = Li, Na, K, . . .). The local structure can be obtained from NMR measurements and is mainly made of so-called Q^3 and Q^4 units [38]. The former corresponds to the usual silica tetrahedron made of one silicon and four Group VI atoms at the corner (e.g. $SiSe_{4/2}$) while the latter has one oxygen atom ionically bonded to the alkali cation (e.g. $SiSe_{5/2}^{\ominus}Na^{\oplus}$) (Fig. 3).

Then, the probabilities can be evaluated for different steps of cluster sizes following the procedure described in the previous sections. It appears that the creation of a $Q^4 - Q^4$ connection leads to a stressed rigid cluster if the number of constraints is computed, while the $Q^4 - Q^3$ and $Q^3 - Q^3$ connections yield respectively isostatically stressed and floppy clusters. The SICA results show again that the intermediate phase shows up if a nonzero fraction of small rings
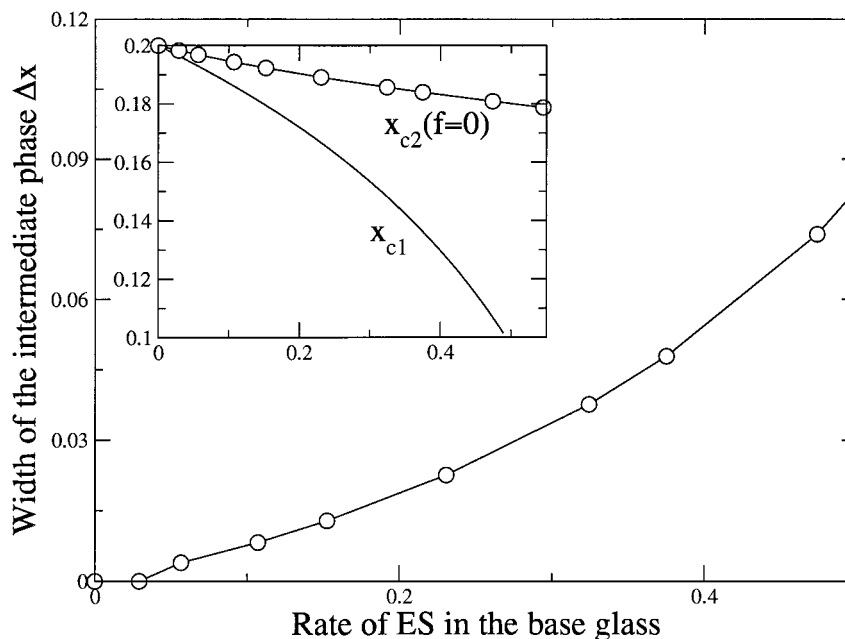
Fig. 4. Width of the intermediate phase Δx as a function of the rate of edge-sharing (ES) in the base glass. The insert shows the solutions x_{c1} and x_{c2} obtained from SICA analysis, again as a function of ES.

is allowed in the structure, as displayed in Fig. 4. Here in contrast with chalcogenides, the glass optimum corresponding to the vanishing of the number of floppy modes represents the upper limit of the intermediate phase, which is consistent with the fact that one starts from an almost stressed rigid molecular network at low modifier concentration. Increase of the alkali content leads to an increase of floppiness. In the oxide system $(1-x)SiO_2 - xM_2O$, the width Δx should be very small or zero since the fraction of ES in the oxide systems is almost zero [20]. Still, percolative effects are expected at the concentration $x = 0.2$ corresponding to the transition from rigid to floppy networks. In sulfur and selenide glasses such as $(1-x)SiO_2 - xNa_2S$, the width should be much broader because of the existence of a high amount of ES tetrahedra in the SiS_2 or $SiSe_2$ base networks [38]. In the sulfur base glass, ^{29}Si NMR have shown that the rate of ES should be about 0.5, slightly higher than in the selenide analogous system [39]. As a result, one should observe a window of about $\Delta x = 0.09$. Unfortunately, results on these systems are available only for an alkali concentration $x > 0.2$ [40]. However, in the different silica-based glasses, a rigidity transition has been observed [41] at the concentration $x = 0.2$, which should provide guidance for forthcoming studies in this area.

Finally, temperature effects should be observable close to this transition. Since the concentration of alkali free carriers n_L depends on the temperature (the higher the temperature, the higher n_L), an increase of the temperature T should lead to a decrease of the number of network constraints, the fraction of intact bond-stretching constraints n_c^α of the alkali atom being proportional to $1 - n_L$. Consequently, a shift of the mechanical threshold ($f = 0$) to the higher concentrations should result from an increase of T.

6. SUMMARY

In this paper, we have shown how stress change in molecular systems can be understood from the combination of cluster construction and constraint counting. We have found that there is a single transition from floppy to rigid networks in a certain number of structural possibilities. An intermediate phase intervenes when a fraction of nonzero molecular isostatic stripes are allowed, which makes this new phase globally stress-free. The similarity of this new phase with the superconducting filamentary phase in HTSC [2] and also in biological networks [13] is striking and should be worked out in more depth in the future.

ACKNOWLEDGMENTS

REFERENCES

1. J. H. Scon, C. Kloc, and B. Batlogg, *Nature (London)* **408,** 549 (2001); J. H. Scon, C. Kloc, and B. Batlogg, *Science* **293,** 2432 (2001).
2. J. C. Phillips, *Phys. Rev. Lett.* **88,** 216401 (2002).
3. J. C. Phillips, *Philos. Mag.* **82,** 783 (2002).
4. T. Schneider and H. Keller, *Phys. Rev. Lett.* **86,** 4899 (2001).
5. V. J. Emery and S. A. Kivelson, *Physica C* **209,** 597 (1993).
6. S. R. Elliott, *Physic of Amorphous Materials* (Wiley, New York, 1989).
7. M. Tatsumisago, B. L. Halfap, J. L. Green, S. M. Lindsay, and C. A. Angell, *Phys. Rev. Lett.* **64,** 1549 (1990).
8. J. C. Phillips, *J. Non-Cryst. Solids* **34,** 153 (1979).
9. J. C. Phillips, *J. Non-Cryst. Solids* **43,** 37 (1981).
10. M. F. Thorpe, *J. Non-Cryst. Solids* **57,** 355 (1983).
11. H. He and M. F. Thorpe, *Phys. Rev. Lett.* **54,** 2107 (1985).
12. U. Senapati and A. K. Varshenya, *J. Non-Cryst. Solids* **185,** 289 (1995); T. Wagner, and S. Kasap, *Phil. Mag. B* **74,** 667 (1996).
13. M. F. Thorpe and P. M. Duxbury, eds. *Rigidity Theory and Applications*, Fundamental Materials Research Series (Plenum Press/Kluwer Academic, New York 1999).
14. X. Feng, W. J. Bresser, and P. Boolchand, *Phys. Rev. Lett.* **78,** 4422 (1997).
15. D. Selvenathan, W. J. Bresser, and P. Boolchand, *Phys. Rev. B* **61,** 15061 (2000).
16. M. F. Thorpe, D. J. Jacobs, M. V. Chubynsky, and J. C. Phillips, *J. Non-Cryst. Solids* **266–269,** 859 (2000).
17. M. Micoulaut, R. Kerner, and D. M. dos Santos-Loff, *J. Phys. Cond. Mat.* **7,** 8035 (1995).
18. R. Kerner and D. M. dos Santos-Loff, *Phys. Rev. B* **37,** 3881 (1988).
19. R. Kerner, K. Penson, and K. H. Bennemann, *Europhys. Lett.* **19,** 363 (1992).
20. F. L. Galeener, D. B. Kerwin, A. J. Miller, and J. C. Mikkelsen Jr., *Phys. Rev. B* **47,** 7760 (1993).
21. M. Micoulaut, *Physica B* **212,** 43 (1995).
22. P. J. Bray, S. A. Feller, G. E. Jellison, and Y. H. Yun, *J. Non-Cryst. Solids* **38/39,** 93 (1980).
23. D. J. Jacobs and M. F. Thorpe, *Phys. Rev. Lett.* **80,** 5451 (1998).
24. M. F. Thorpe, D. J. Jacobs, and M. V. Chubynsky, in *Rigidity Theory and Applications*, M. F. Thorpe, and P. M. Duxbury, eds. (Plenum Press/Kluwer Academic, New York, 1999), p. 239.
25. D. S. Franzblau and J. Tersoff, *Phys. Rev. Lett.* **68,** 2172 (1992).
26. P. Boolchand and W. J. Bresser, *Philos. Mag. B* **80,** 1757 (2000).
27. P. Boolchand and M. F. Thorpe, *Phys. Rev. B* **50,** 10366 (1994).
28. Y. Wang, P. Boolchand, and M. Micoulaut, *Europhys. Lett.* **52,** 633 (2000).
29. M. Micoulaut, *J. Mol. Liquids* **71,** 107 (1997).
30. Z. Jinfeng and S. Mian-Zeng, *Materials for Solid state batteries*, B. V. R. Chowdari and S. Radhakrishna, eds. (1986), p. 487.
31. S. W. Martin, *Eur. J. Solid. St. Inorg. Chem.* **28,** 163 (1991).
32. S. W. Martin, J. A. Sills, *J. Non-Cryst. Solids* **135,** 171 (1991).
33. S. Sahami, S. Shea, and J. Kennedy, *J. Electrochem. Soc.* **132,** 985 (1985).
34. M. Zhang and P. Boolchand, *Science* **266,** 1355 (1994).
35. R. Kerner , and J. C. Phillips, *Solid State Comm.* **117,** 47 (2000).
36. L. F. Perondi, R. J. Elliott, R. A. Barrio, and K. Kaski, *Phys. Rev. B* **50,** 9868 (1994).
37. J. F. Stebbins, *J. Non-Cryst. Solids* **106,** 359 (1988).
38. H. Eckert, J. Kennedy, A. Pradel, and M. Ribes, *J. Non-Cryst. Solids* **113,** 187 (1989).
39. A. Pradel, V. Michel-Liedos, M. Ribes, and E. Eckert, *Chem. Mater.* **5,** 377 (1993).
40. A. Pradel, J. Taillades, M. Ribes, and H. Eckert, *J. Non-Cryst. Solids* **188,** 75 (1995).
41. Y. Vaills, G. Hauret, and Y. Luspin, *J. Non-Cryst. Solids* **286,** 224 (2001).
42. M. S. Osofsky, R. J. Soulen, J. H. Claasen, G. Trotter, H. Kim, and J. S. Horowitz, *Phys. Rev. Lett.* **87,** 197004 (2001).